

Achievements and Continued New Phase of the Large Helical Device

Hiroshi YAMADA for LHD Experiment Group

National Institute for Fusion Science, 322-6 Oroshi, Toki, Gifu 509-5292, Japan

(Received: 17 November 2009 / Accepted: 19 January 2010)

This paper reviews major achievements in the large helical device (LHD) project and discusses the prospects in the upcoming nearest future. The LHD is the largest magnetic confinement device among diversified helical systems and employs superconducting coils. These significant features have enabled comprehensive studies on steady-state net-current free plasmas with plasma parameters comparable to large tokamaks. The major achievements are highlighted by high beta (5.1%), high density ($1.2 \times 10^{21} \text{m}^{-3}$), high ion temperature (T_i of 5.6 keV at $1.6 \times 10^{19} \text{m}^{-3}$), and steady-state operation (3200 s with 490 kW). This progress in physical parameters has elucidated the potential of net-current free helical plasmas for an attractive fusion reactor. The recent finding of an internal diffusion barrier has extended high density operation beyond $1 \times 10^{21} \text{m}^{-3}$ at the moderate magnetic field of 2.5 T. This achievement provides a novel scenario to a super high density reactor. Based on achievements that have resolved fundamental concerns in helical system, an upgrade plan to advance the LHD project to a new phase has just started. Major elements are a closed divertor system to improve particle control under high heating power and steady state, upgrade of heating capability and the use of deuterium gas.

Keywords: heliotron, superconducting system, steady state operation, high β , high density, internal diffusion barrier, impurity hole, 3-D effect

1. Introduction

The large helical device (LHD) is the world largest toroidal device for studying the physics of a net current-free plasmas. LHD is based on the concept of a heliotron magnetic field and employs superconducting coils [1,2]. The progress of the LHD project is reviewed putting emphasis on the latest achievements.

The role of LHD can be revealed by recalling the definition of the broader approach. The basic activities and functions in a broader approach are categorized into three frameworks which are primarily ITER oriented, ITER/DEMO oriented and primarily DEMO oriented. This second category, ITER and DEMO oriented, is attributed to exploration of operational regimes and issues complementary to those addressed in ITER. Here three major subjects have been extracted; steady state operation, the advanced plasma regime that is high β , and control of power fluxes to walls. Although these are identified in the roadmap towards a tokamak DEMO reactor, it should be pointed out that these are indeed what are defined as the main mission of LHD at the beginning of the project. Therefore the LHD project is aimed at two goals, one is to formulate a systematic scenario to an attractive helical reactor and one is a comprehensive understanding of toroidal plasmas including tokamaks.

2. Machine Status and Parametric Progress

LHD has worked very well for 12 years since its initial operation in 1998 [3]. The accumulation of

operational experience over 12 years proves that LHD has built up the engineering base of a large-scale superconducting and cryogenic system for fusion reactor development [4].

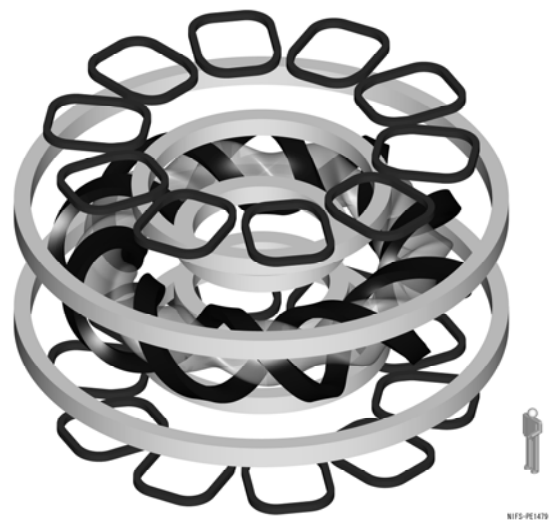


Fig.1 A bird's eye view of the LHD magnet system.

LHD is based on the heliotron magnetic configuration [5] and has a pair of helical coils and 3 sets of poloidal coils (see Fig.1). All these coils are superconducting and generate the confining magnetic field without the help of net plasma current. In addition, LHD has 10 pairs of perturbation coils which enable the study of resonant magnetic perturbations [6]. NBI is the primary heating

source and also ECH as well as ICH play important roles in the experiment. The major operating specifications of LHD are summarized in Table I.

Table I Machine specifications of LHD

Major radius	3.9 m
Minor radius of helical coil	0.975 m
Minor radius of plasma	0.5 – 0.65 m
Magnetic field	2.96 T at $R = 3.6$ m
Magnetic energy	0.77 GJ
Coil temperature	3.5 K
Heating power	
ECH	3.5 MW
ICH	3.0 MW
NBI	23 MW

Several-month-long operation has been executed 12 times since 1998. The 13th experimental campaign was conducted in 2009. The operational time of the helium compressor has amounted to 57,000 hours with the average duty of 99.4%. The superconducting coils have been excited more than 1,300 times and LHD has produced more than 94,000 plasma discharges to date. This unusually high availability is due to a reliable superconducting system and the intrinsic advantages of net current free plasmas.

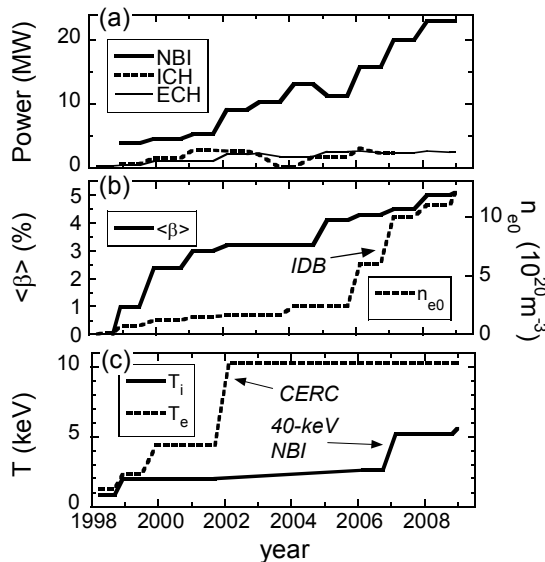


Fig.2 Progress of heating capability and representative plasma parameters. (a) heating power, (b) volume averaged β and the central electron density, and (c) central ion and electron temperature.

Figure 2 is an overview of the progress in these 11 years. Diversified achievements have been obtained by a synergetic effect of technological upgrade and new physics findings. The superconducting coils provide a reliable

steady state magnetic field. Heating capability has been growing, in particular NBI. Due to this firm engineering foundation, physical parameters have progressed dramatically. The steady-state heating facility of ICH [7] as well as ECH makes an essential contribution to a 1-hour long discharge. The beta and the central density are plotted in the middle in Fig.2(b). Distinguished development of the central density is due to the finding of an internal diffusion barrier (IDB) [8,9] describe later. The progress of temperatures is drawn in Fig.2(c). The electron temperature jumped up by the improved confinement due to radial electric field, which is referred to a core electron root confinement (CERC) [10]. The ion temperature has begun to increase recently due to a perpendicular NBI [11] which is favorable to ion heating because of a low accelerating voltage of 40 keV.

3. Steady State Operation

LHD has already achieved a one-hour long steady-state discharge with the temperatures in the keV range as shown in Fig.3. The total amount of input energy reached 1.6 GJ [12]. This steady state operation of LHD is highlighted by 500 kW which consists of 400 kW of ICH and 100 kW of ECH. As shown in Fig. 3(d), the temperature of divertor plates is saturated by a magnetic axis swing technique [13]. A sweep of only 3cm in major radius of the magnetic axis position (less than 1% of the major radius of the LHD) was sufficient to disperse the divertor heat load.

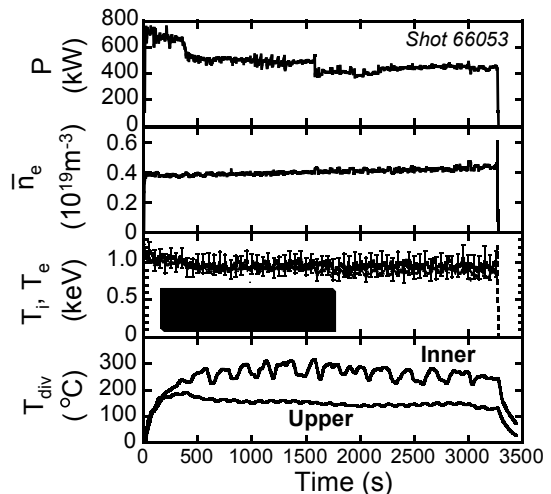


Fig.3 Waveforms of a typical steady-state long-pulse discharge in LHD. (a) heating power, (b) line averaged density, (c) temperatures, and (d) temperature of divertor plate. This figure is a reproduction from Fig.9 in H.Yamada et al., Fusion Eng. Design 84 (2009) 186.

The RF oscillator for ICH itself has already achieved 1.6 MW operation for 5000 s [7]. Also the steady state

heating capability of ECH is now upgraded to 300 kW. Together with a new closed divertor system with more efficient heat removal than the present one, further upgrade of the steady state heating capability will enable 3 MW operation for one hour which corresponds to an input energy of 10 GJ. This is close to the ITER regime in terms of handled auxiliary heating.

4. High Beta

The development of beta in the LHD experiment is very encouraging. The volume averaged β of 5 % has been achieved without any disastrous instability while MHD activity is certainly seen as theory predicts [14]. The high beta ranging up to 5 % is maintained for longer than 100 times the energy confinement time. The LHD experiment has discovered that the interchange instability in the magnetic hill is benign [15,16]. The interchange mode analysis based on the linear MHD theory suggests that LHD plasmas reaching 5% are unstable against the interchange mode due to a magnetic hill. In spite of this unfavorable stability condition, the plasma can pass through the unstable region and evolves to the high β state. Figure 4 indicates that the achievable beta is limited by the available heating power without a hard beta limit. Geometrical optimization and the upgrade of the heating power will enable further development.

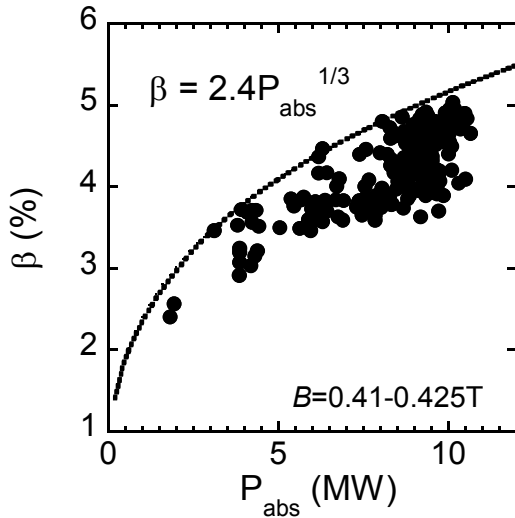


Fig.4 Achieved β as a function of the absorbed heating power.

5. High Density

The assessment of the density limit is extremely important in the operational design of a reactor. In tokamaks, the operational density limit is well described by the Greenwald limit [17]. In contrast, the plasma in LHD can be operated well beyond this limit when the dependence on the plasma current density is rephrased by the rotational transform. Another scaling of the density limit for helical systems has been proposed by Sudo [18],

which is essentially proportional to the square root of power density. This scaling is applicable to LHD for diversified density profiles when we take the edge density at the electron temperature of 100 eV [19]. Figure 5 shows the dependence of density on the heating power. The case with the pellet injection is a more peaked density profile than the case with normal gas-puffing. The offset between the cases with different fueling schemes as well as the scatter of data converges when the local edge density at the electron temperature of 100 eV is evaluated (see Fig.5 (b)).

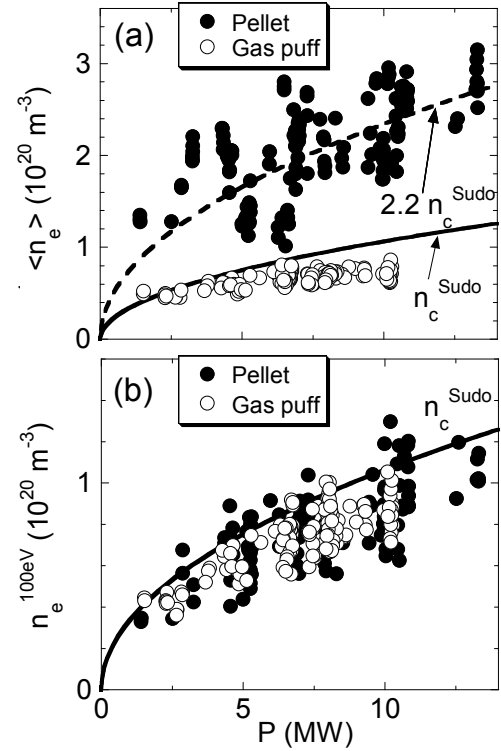


Fig.5 Dependence of operational envelope of density for the cases with different fueling schemes on heating power. (a) volume averaged density and (b) edge density at the electron temperature of 100 eV.

This means that the core density is free from operational limit. This advantage over tokamaks is due to the freedom from current drive and disruption. Then the chance to investigate the underlying physics of the density limit, which is not determined by current disruption, becomes available. Also, since the energy confinement time of helical systems has significant positive dependence on density like $\tau_E \propto \bar{n}_e^{0.6}$ [20], extension of this favorable density dependence is a very important issue for the prospects of a fusion reactor.

As a highlight of the high density topic, a distinguished high density plasma in LHD should be noted. After a sequence of pellet injections to build up the central

density [21], the super-dense-core is formed under the condition of reduced edge recycling and avoidance of the local concentration of neutrals. The plasma exhibits a high peaked density profile which is referred to an internal diffusion barrier (IDB) [8,9]. Although the plasma with an IDB has a much higher density in the core than the gas-fuelled plasma, the electron temperature is even higher. Then the central pressure is enhanced by a factor of 4. By this operation the central density has reached $1.2 \times 10^{21} \text{m}^{-3}$ at the moderate magnetic field of 2.5 T. This recent discovery suggests a potential for the novel scenario of a super high density reactor with ignition at relatively low temperatures less than 10 keV.

6. High Ion Temperature Mode

Recently a perpendicular NBI with a low accelerating voltage of 40 keV has become available and ion heating experiments have progressed. The previous tangential NBI has a higher accelerating voltage of 180 keV, which predominantly heats electrons. To date the central ion temperature of 5.6 keV has been achieved at the density of $1.6 \times 10^{19} \text{m}^{-3}$ as shown in Fig.6. The ion temperature profile is peaked and higher than the electron temperature in the core.

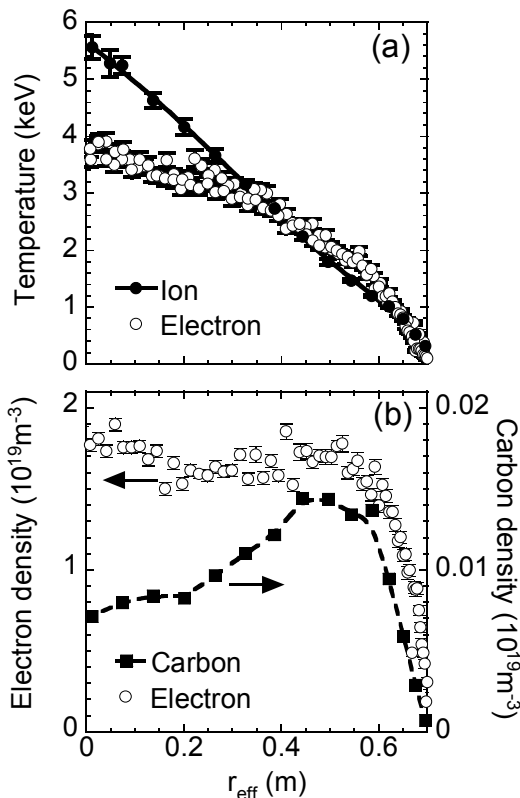


Fig.6 Typical profiles in the high-ion-temperature plasma. (a) ion and electron temperatures and (b) electron and carbon densities.

A distinguished feature is observed in the ion temperature in the core relative to the peripheral

temperature. While the peripheral temperature remains low in spite of an increase of heating power, the central temperature dramatically grows. The power degradation of heat transport, in other words temperature dependence, is significantly mitigated in this mode [22].

In addition, it is very interesting that this high ion temperature mode is accompanied by a so called impurity hole [23]. Figure 6 (b) shows the typical profiles of electron density by open circles and carbon impurity density by closed squares. It should be noted that the scales differ by 100 times. The profile of the carbon impurity is extremely hollow compared with the electron density profile. This trend is emphasized by the increase of the ion temperature gradient. Therefore even with carbon impurity pellet injection, carbon is expelled from the core with significant outward convection. It should be noted that this phenomena contradicts the prediction of neoclassical transport with an observed negative radial electric field.

7. 3-D Effect

It should be pointed out that the 3-D equilibrium has the distinguished features of a magnetic island and stochastic field. The numerical code HINT [24] that copes with this 3-D equilibrium appropriately has been developed in NIFS. Figure 7 (a) is the pressure profile in a typical high- β discharge. The open circles are the experimental values and the dotted curve is the result from HINT [25]. HINT reconstructs the plasma equilibrium quite well, nonetheless, controversial observation comes out. It is that a significant pressure gradient exists in the edge stochastic area. It should be pointed out that a 3-D equilibrium is not specific to helical systems. Resonant magnetic field coils are considered in tokamaks so as to control ELMs and also stabilize the RWM.

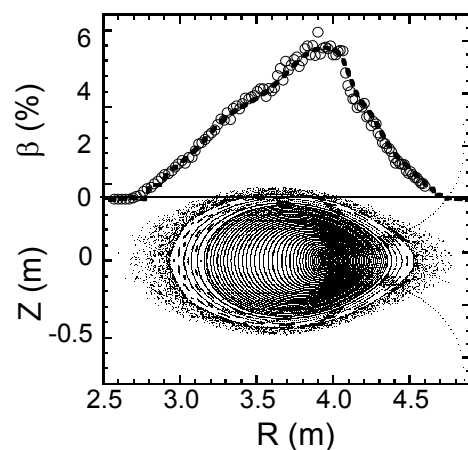


Fig.7 (a) Pressure (β) profile. Open circles are experimental values and dotted curve is the result from HINT. (b) Reconstructed equilibrium by HINT.

There are possibilities that a plasma heats the

stochastic magnetic field spontaneously or that a finite pressure gradient is determined consistently with the characteristics of a stochastic magnetic field.

With regard to heat transport due the stochastic magnetic field, the Rechester-Rosenbluth model [26] is well known, but it predicts unusually large radial transport at high electron temperatures in LHD. Here the diffusion coefficient of the magnetic field line D_{FL} is an essential parameter. The Rechester-Rosenbluth model assumes a simple Markov chain process, however the stochastic area in LHD has a memory of the structure of the magnetic island. In this situation D_{FL} is defined as the island width squared divided by the parallel length around a circumference in the magnetic island. As temperature increases, the parallel length increases. And consequently D_{FL} is reduced. Then a finite pressure gradient can be expected in the stochastic area [27]. The 3-D edge transport simulation in the stochastic area by the EMC3-EIRENE code [28,29] supports this scenario. As the electron temperature increases, the electron temperature in the island is flattened more clearly and the boundary becomes clearer and extends. This change corresponds to the fact that the parallel path becomes predominant.

8. Nearest Future Plan and Summary

In 2010, LHD will make a significant step forward. The new 5th NBI with perpendicular injection and a power of 7MW will be available. The total heating power by NBI will reach 30 MW. Also the vacuum vessel will be modified in order to incorporate a baffle structure to form a closed divertor. As the first step, the closed divertor will be installed at the inboard side of 2 of 10 toroidal sections. This is a proto-type without cryo-pumps. The capability of neutral compression will be evaluated and it will be applied to the final design. Together with this closed divertor, an upgrade of the steady state heating capability of ICH as well as ECH will enable us to attempt steady state operation with 3MW for 1 hour in a couple of years. The deuterium experiment is also a very important next step to assess the isotope effect. Reactor design studies are also progressing based on the results from LHD.

It is worth mentioning the Asian network, in other words, the solidarity of superconducting steady state toroidal experiments. 5 world-class major superconducting experiments; LHD, EAST [30], KSTAR[31], SST-1[32] and JT-60SA [33], are working or under construction in Asia. It should be realized that a significant gap exists between these present experiments and the next generation; ITER. Therefore it is extremely important to share common critical issues among these experiments and collaboration can accelerate the progress. It should be emphasized that a complementary approach provides a more mature solution than one line alone.

LHD has been providing the “unique” and “complementary” basis in fusion power development and shares the role with tokamaks. Recent highlights of physics achievements are reviewed in this article. The understanding of net current free plasmas has progressed dramatically through LHD experiments. Highlighted achievements and accurate knowledge about steady state operation, high β , density limit and 3-D effect are complementary to tokamaks in fusion power development. The near-term upgrade package including a closed helical divertor, the upgrade of heating capability, and deuterium will reinforce the role of LHD. In the coming next decade, LHD is aimed at the challenging integration of elements towards an attractive fusion reactor.

Acknowledgements

The author is grateful to all contributors to the LHD project, in particular colleagues in the LHD experiment group. The support by the LHD operation group is greatly appreciated. This work is supported by budget NIFS09ULGG001 of the National Institute for Fusion Science.

References

- [1] A. Iiyoshi *et al.*, Nucl. Fusion **39**, 1245 (1999) .
- [2] O. Motojima *et al.*, Nucl. Fusion **40**,599 (2000).
- [3] H.Yamada *et al.*, Fusion Eng. Design **84**, 186 (2009).
- [4] T. Mito *et al.*, Fusion Eng. Des. **81**, 2389 (2006).
- [5] K.Uo, Plasma Phys. **13**, 243 (1971)
- [6] A. Komori *et al.*, Nucl. Fusion **45**, 837 (2005)
- [7] T. Seki *et al.*, Fusion Sci. Technol. **40**, 253 (2001).
- [8] N. Ohyabu *et al.* Phys. Rev. Lett. **97**, 05502 (2006).
- [9] H.Yamada *et al.*, Plasma Phys. Control. Fusion **49**, B487(2007)
- [10] M.Yokoyama *et al.*, Nucl. Fusion **47**, 1213 (2007)
- [11] Y. Takeiri *et al.*, Nucl. Fusion **47**, 1078 (2007)
- [12] T. Mutoh *et al.*, Nucl. Fusion **47**, 1250 (2007)
- [13] H.Ogawa *et al.*, Plasma Fusion Res. **2**, 043 (2007)
- [14] S.Sakakibara *et al.*, Plasma Phys. Control. Fusion **50**, 124014 (2008).
- [15] H.Yamada *et al.*, Plasma Phys. Control. Fusion **41**, A55 (2001).
- [16] K.Y. Watanabe *et al.*, Nucl Fusion **45**, 1247 (2005).
- [17] M.Greenwald *et al.*, Nucl. Fusion **28**, 2199 (1988)
- [18] S.Sudo *et al.*, Nucl. Fusion **30**, 11 (1990)
- [19] J.Miyazawa *et al.*, Nucl. Fusion **48**, 015003 (2008).
- [20] H.Yamada *et al.*, Nucl. Fusion **45**, 1684 (2005)
- [21] R.Sakamoto *et al.*, Plasma Fusion Res. **2**, 047 (2007).
- [22] K.Ida *et al.*, Nucl. Fusion **49**, 095024 (2009).
- [23] M.Yoshinuma *et al.*, Nucl. Fusion **49**, 062002 (2009)
- [24] K.Harafuji *et al.*, J.Comput. Phys. **81**, 123 (1989)
- [25] K.Y.Watanabe *et al.*, Plasma Phys. Control. Fusion **49**,

- 605 (2007).
- [26] A.B.Rechester and M.N.Rosenbluth, Phys. Rev. Lett. **40**, 38 (1971).
- [27] M.Kobayashi *et al.*, J. Nucl. Mater. **363-365**, 294 (2007).
- [28] Y.Feng *et al.*, Contrib. Plasma Phys. **44**, 57 (2004).
- [29] D.Reiter *et al.*, Fusion Sci. Technol. **47**, 172 (2005).
- [30] B.Wan *et al.*, Nucl. Fusion **49**, 104011 (2009).
- [31] Y.K.Oh *et l.*, Fusion Eng. Design **83**, 804 (2008).
- [32] B.Sarkar *et al.*, Fusion Eng. Design **81**, 2633 (2006).
- [33] M.Matsukawa *et al.*, Fusion Eng. Design **83**, 795 (2008).